Int. J. Solids Structures Vol. 30, No. 12, pp. 1649–1662, 1993
Printed in Great Britain

0020–7683/93 $6.00+ .00

POSTBUCKLING OF INFINITE LENGTH CYLINDRICAL PANELS UNDER COMBINED THERMAL AND PRESSURE LOADING

TANCHUM WELLER and IGOR PATLASHENKO
Faculty of Aerospace Engineering, Technion—Israel Institute of Technology, Haifa 32000, Israel

(*Received* 1 *April* 1992)

Abstract—An analysis for the pre- and postbuckling behavior of infinite length panels, stiffened and unstiffened, including transverse shear and temperature dependent elastic moduli and thermal expansion coefficients, is proposed. The analysis involves the solution of a system of nonlinear differential equations by means of a relatively new spline-collocation method. Results, yielded by the present study and describing the response of lightly to moderately stringer-stiffened panels and unstiffened ones, subjected to heating and pressure loading, are presented. It is shown that neglect of transverse shear and temperature effects may lead to erroneous results and conclusions.

1. INTRODUCTION

Reusable hypersonic flight vehicles are subjected to combined aerothermal and mechanical loading. Broad reviews on the progress and state-of-the-art in the area of hypersonic structures and materials are given in Jackson *et al.* (1987), Tenney *et al.* (1988) and Thornton (1990). The complicated coupling between the aerodynamic flow field and the structural heat transfer, the aerothermostructural problem, is dealt with in numerous papers [e.g. Thornton *et al.* (1989), Thornton and Dechaumphai (1987), Shih *et al.* (1988) and Wieting *et al.* (1988)].

Unstiffened and stiffened thin-walled cylindrical type elements are considered as prime candidates for the airframe of hypersonic vehicles. These structures are, however, susceptible to buckling instability. Therefore, their introduction as efficient weight/stiffness load carrying structural elements, depends strongly upon the capability to predict adequately their incipient buckling, and particularly their transient response from the critical buckling state to an adjacent postbuckled equilibrium state and the postbuckling behavior thereafter. This is because the behavior determines the "sensitivity" of the panel to the presence of initial geometrical imperfections, i.e. either its failure, usually of a catastrophic nature, under loads which are lower than its critical load, or its capability to sustain safely loads which follow a postbuckling equilibrium path, thus contributing to the increase in element structural efficiency.

Buckling and postbuckling of cylindrical panels and shells, stiffened and unstiffened, under mechanical type loading, has been the subject of hundreds of studies. Studies on thermoelastic stability problems are also quite extensive [see Keene and Hetnarsky (1990) and the many references cited there and Ziegler and Rammerstorfer (1989)]. However, it should be noted that in so far as postbuckling due to thermal loading is considered, only initial buckling or "narrow" postbuckling is dealt with in most of the investigations, i.e. just after incipient buckling occurs.

There are various approaches to treating the stability problem. The traditional approach is based on linearization of the prebuckling state, thus reducing mathematical complexities. Such an approach renders acceptable results for a wide range of problems, where bending in the prebuckling state can be discarded. In structures, however, which exhibit pronounced nonsymmetric deformation, this type of solution is inadequate. There, an approach, which treats the stability problem as a nonlinear boundary problem for all states of loading, pre- and postbuckling, is more appropriate and therefore its application for this class of problems is preferable [see Andreev *et al.* (1988)]. Such solutions provide the means for investigation of cases where nonunique states of equilibrium exist to determine

bifurcation and limit loads and to describe the behavior in the postbuckling range. It should be noted that in the above approaches the structures are considered as being relatively thin and therefore the transverse shear is usually not accounted for.

The design of aerothermal structures involves application of a new generation of materials. Utilization of these materials may result, amongst others, in anisotropy of the structural elements, substantial temperature dependence of their properties and low transverse shear stiffness. Neglecting these properties, even when applying linear type analysis, may lead to faulty results (Khoroshun *et al.*, 1988a, b). Therefore, the design of thin-walled constructions for "hot" type structures calls for the introduction of nonlinear approaches, accounting for the above mentioned properties, for their analysis.

The above discussion obviously emphasizes the need to provide an improved analytical tool, which accounts for temperature dependent material properties as well as transverse shear effects, for better prediction of buckling and description of postbuckling behavior of thin-walled hypersonic type cylindrical elements, subjected to combined thermal and mechanical loading. As a step aiming towards achieving this goal it is the objective of the present study to develop a tool for the investigation of buckling and postbuckling of infinitely long cylindrical panels, fabricated from materials characterized by temperature dependent moduli of elasticity and coefficients of thermal expansion, that considers transverse shear flexibility effects.

2. ANALYSIS

A Timoshenko type geometrically nonlinear model constitutes the basis for the present analysis. The equations (Grigorenko and Timonin, 1982) which govern the behavior of the cylindrical panel treated herein, are given by the following kinematic relations:

$$\varepsilon_{11}=\frac{\partial u}{\partial\alpha_1}+\frac{1}{2}\left(\frac{\partial w}{\partial\alpha_1}\right)^2,\quad \varepsilon_{12}=\frac{1}{R}\frac{\partial u}{\partial\alpha_2}+\frac{\partial v}{\partial\alpha_1}+\frac{1}{R}\left(\frac{\partial w}{\partial\alpha_1}\cdot\frac{\partial w}{\partial\alpha_2}-v\cdot\frac{\partial w}{\partial\alpha_1}\right),$$

$$\varepsilon_{22}=\frac{1}{R}\left(\frac{\partial v}{\partial\alpha_2}+w\right)+\frac{1}{2R^2}\left(v^2+\left(\frac{\partial w}{\partial\alpha_2}\right)^2-2v\cdot\frac{\partial w}{\partial\alpha_2}\right),\quad \kappa_{11}=\frac{\partial\psi_1}{\partial\alpha_1},$$

$$2\kappa_{12}=\frac{1}{R}\frac{\partial\psi_1}{\partial\alpha_2}+\frac{\partial\psi_2}{\partial\alpha_1}-\frac{1}{R^2}\frac{\partial u}{\partial\alpha_2},\quad \kappa_{22}=\frac{1}{R}\left(\frac{\partial\psi_2}{\partial\alpha_2}-\frac{1}{R}\frac{\partial v}{\partial\alpha_2}-\frac{1}{R}w\right),$$

$$\theta_1=-\frac{\partial w}{\partial\alpha_1},\quad \theta_2=\frac{1}{R}\left(-\frac{\partial w}{\partial\alpha_2}+v\right),$$

$$\varepsilon_{13}=\psi_1-\theta_1,\quad \varepsilon_{23}=\psi_2-\theta_2, \tag{1}$$

equilibrium equations:

$$\frac{\partial N_1}{\partial\alpha_1}+\frac{1}{R}\frac{\partial N_{12}}{\partial\alpha_2}-\frac{1}{R^2}\frac{\partial M_{12}}{\partial\alpha_2}+q_1^*=0,$$

$$\frac{\partial N_{12}}{\partial\alpha_1}+\frac{1}{R}\frac{\partial N_2}{\partial\alpha_2}+\frac{1}{R}Q_2+q_2^*=\frac{1}{R}\left(N_{12}\cdot\theta_1+\left(N_2+\frac{1}{R}M_2\right)\theta_2\right),$$

$$\frac{\partial Q_1}{\partial\alpha_1}+\frac{1}{R}\frac{\partial Q_2}{\partial\alpha_2}-\frac{1}{R}N_2+q_3^*=\frac{\partial}{\partial\alpha_1}(N_1\cdot\theta_1+N_{12}\cdot\theta_2)+\frac{1}{R}\frac{\partial}{\partial\alpha_2}\left(N_{12}\cdot\theta_1+\left(N_2+\frac{1}{R}M_2\right)\theta_2\right),$$

$$\frac{\partial M_1}{\partial \alpha_1}+\frac{1}{R}\frac{\partial M_{12}}{\partial \alpha_2}-Q_1=0, \quad \frac{\partial M_{12}}{\partial \alpha_1}+\frac{1}{R}\frac{\partial M_2}{\partial \alpha_2}-Q_2=0, \tag{2}$$

and relations for the force and moment resultants:

$$\begin{aligned}
N_1 &= C_{11}\varepsilon_{11}+C_{12}\varepsilon_{22}+K_{11}\kappa_{11}+K_{12}\kappa_{22}-N_{1T},\\
N_2 &= C_{12}\varepsilon_{11}+C_{22}\varepsilon_{22}+K_{12}\kappa_{11}+K_{22}\kappa_{22}-N_{2T},\\
N_{12} &= C_{66}\varepsilon_{12}+K_{66}\cdot 2\kappa_{12}+\frac{1}{R}(K_{66}\varepsilon_{12}+D_{66}\cdot 2\kappa_{12}),\\
M_1 &= K_{11}\varepsilon_{11}+K_{12}\varepsilon_{22}+D_{11}\kappa_{11}+D_{12}\kappa_{22}-M_{1T},\\
M_2 &= K_{12}\varepsilon_{11}+K_{22}\varepsilon_{22}+D_{12}\kappa_{11}+D_{22}\kappa_{22}-M_{2T},\\
M_{12} &= K_{66}\varepsilon_{12}+D_{66}\cdot 2\kappa_{12},\\
Q_1 &= C_{13}\varepsilon_{13},\\
Q_2 &= C_{23}\varepsilon_{23},
\end{aligned} \tag{3}$$

where α_1 is the longitudinal coordinate, α_2 is the circumferential angle, R is the radius and u, v, w are displacement components of the coordinate surface (Fig. 1); ψ_1, ψ_2 are the angles of rotation of a segment, originally normal to the coordinate surface in planes $\alpha_2 = \text{const}$ and $\alpha_1 = \text{const}$, respectively; N_1, N_2, N_{12}, M_1, M_2, M_{12}, Q_1, Q_2 are the in-plane force, moment and shear force resultants; q_1^*, q_2^*, q_3^* are the projections of external surface load onto axes associated with the undeformed coordinate surface. (When the acting load remains directed along the normal to the coordinate surface in the deformed state, then $q_1^* = q(\alpha_1,\alpha_2)\cdot\theta_1$, $q_2^* = q(\alpha_1,\alpha_2)\cdot\theta_2$, $q_3^* = q(\alpha_1,\alpha_2)$, where θ_1, θ_2 are the angles of rotation of the normal to the coordinate surface.)

In eqns (3) the coefficients C_{ij}, K_{ij}, D_{ij} are the structural stiffnesses and N_{iT}, M_{iT} are the thermal forces and moments, respectively. The stiffnesses are given by the following integrals:

$$\begin{aligned}
C_{ij} &= \int_{-h_2}^{h_1} E_{ij}\,dz, \quad K_{ij} = \int_{-h_2}^{h_1} E_{ij}\cdot z\,dz, \quad D_{ij} = \int_{-h_2}^{h_1} E_{ij}\cdot z^2\,dz,\\
C_{66} &= \int_{-h_2}^{h_1} G_{12}\,dz, \quad K_{66} = \int_{-h_2}^{h_1} G_{12}\cdot z\,dz, \quad D_{66} = \int_{-h_2}^{h_1} G_{12}\cdot z^2\,dz,\\
C_{i3} &= \frac{5}{6}\int_{-h_2}^{h_1} G_{i3}\,dz \quad (i,j=1,2)
\end{aligned} \tag{4}$$

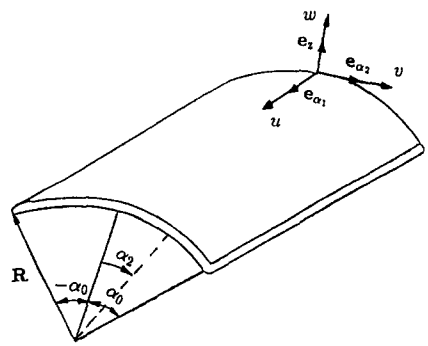

Fig. 1. Geometry of a cylindrical panel.

and the thermal forces and moments are defined by:

$$N_{iT} = \int_{h_2}^{h_1} (E_{1i}\alpha_1^* + E_{i2}\alpha_2^*) \cdot T \, dz,$$

$$M_{iT} = \int_{h_2}^{h_1} (E_{1i}\alpha_1^* + E_{i2}\alpha_2^*) \cdot Tz \, dz \quad (i = 1, 2), \tag{5}$$

where $E_{ii} = E_i/(1 - \nu_{12}\nu_{21})$, $E_{12} = E_{11} \cdot \nu_{12}$ and h_1, h_2 are the distances from the coordinate surface to the upper and lower lateral surfaces of the panel, respectively; $T(\alpha_1, \alpha_2, z)$ is the temperature change from a reference state, and integration is to be performed over the thickness, taking into account the dependence upon T of material properties.

It is worthwhile noting that even for a constant thickness structure, when the coordinate surface coincides with the middle one, the coefficients K_{ij} are not equal to zero, if the temperature dependencies of $E_i(T)$ and $G_{ij}(T)$ are taken into account and temperature distribution is nonsymmetric across the thickness.

The following dependence upon temperature of the elastic moduli E_i, G_{ij}, and the coefficients of linear temperature expansion of α_i^* are assumed:

$$E_i = E_{i0}(1 - b_{1i} \cdot T - b_{2i} \cdot T^2), \quad G_{i3} = G_{i30}(1 - g_{1i} \cdot T - g_{2i} \cdot T^2),$$
$$\alpha_i^* = \alpha_{i0}(1 - l_{1i} \cdot T - l_{2i} \cdot T^2) \quad (i = 1, 2), \tag{6}$$

where b_{ij}, g_{ij}, l_{ij} are constants determined experimentally. Also, it is assumed that Poisson ratios, ν_{ij}, depend only slightly upon temperature and therefore are considered as being constants.

For application of the spline-collocation method, described in Section 3, for the calculation of the behavior of the infinite cylindrical panel, it is convenient to present the equilibrium equations by the kinematic unknown functions u, v, w. Assuming that q and T do not depend upon the α_1 coordinate, inserting (1) into (3) and further into (2), taking into account the stiffnesses variation along α_2 and discarding terms which have derivatives with respect to α_1 a system of three nonlinear ordinary equations is obtained. This can be written in the following matrix-operator form

$$|\Delta_{ij}|_{i,j=1}^{3} \cdot \mathbf{t} = \mathbf{F}(\mathbf{t}), \tag{7}$$

where $\mathbf{t}^T = (t_1 = v, t_2 = w, t_3 = \psi_2)$, and the operators Δ_{ij} and nonlinear functions F_i are given in the Appendix.

The system of equations (7), together with appropriate boundary conditions, constitute a one-dimensional boundary problem. In what follows, two types of boundary conditions at the edges $\alpha_2 = \pm\alpha_0$ will be considered:

(a) clamped ends: $v = w = \psi_2 = 0$,

(b) simply-supported ends: $v = w = M_{22} = 0$. (8)

In the present analysis the problem formulation and the solution method are presented so as to include and treat panels with nonuniform stiffness, due to either variable thickness (e.g. stiffeners), or to uneven temperature distributions when temperature dependence of material properties is accounted for. Also, the proposed analytical model accounts for transverse shear effects, which are usually omitted from "classical" type calculations. In order to achieve an accurate decription of the panel response nonlinear prebuckling deformations are included, and both pre- and postbuckling analyses are regarded as a single nonlinear boundary problem in accordance with Andreev *et al.* (1988).

3. SOLUTION

A relatively new spline-collocation method (Zav'yalov *et al.*, 1980) is employed for the solution of the nonlinear equations (7), together with the boundary conditions (8). The method is based on satisfying the differential system and boundary conditions in a finite set of discretization points. B-splines are adopted to represent the solution vector **t** [eqns (7)].

A subdivision δ is prescribed on the interval $[-\alpha_0, \alpha_0]$: $-\alpha_0 = x_0 < x_1 < \cdots < x_{2N} < x_{2N+1} = \alpha_0$. This subdivision with the additional nodes $x_{-3} < x_{-2} < x_{-1} < x_0 = -\alpha_0$ and $x_{2N+4} > x_{2N+3} > x_{2N+2} > x_{2N+1} = \alpha_0$, which can be chosen rather arbitrarily, yields a subdivision δ'. In accordance with Zav'yalov *et al.* (1980), a system of functions $B_i(x)$ $(i = \overline{-1, 2N+2})$, shown in Fig. 2, is introduced for δ'. This system constitutes a system of normalized local cubic B-splines which forms a basis for the space $S_{3,1}(\delta)$ of twice continuously differential cubic splines constructed in the subdivision δ. Now, a modified scheme in which collocation points y_i are selected in a special way so that they do not coincide with nodes of B-splines $([y_{2i}, y_{2i+1}] \subset [x_{2i}, x_{2i+1}]$, $i = \overline{0, N})$, is applied for the solution of the problem.

Thus, solution of the boundary problem [eqns (7) and (8)] in the interval $[-\alpha_0, \alpha_0]$ is sought in the form of the following expansions:

$$t_j = \sum_{i=-1}^{2N+2} b_i^{(j)} \cdot B_i(x) \quad (j = 1, 2, 3). \tag{9}$$

Inserting (9) into (7), we obtain at the collocation points:

$$\sum_{j=1}^{3} \sum_{m=-1}^{2} [b_{2p+m}^{(j)} \Delta_{ij}(B_{2p+m}(y_{2p}))] = F_i(y_{2p}, b_{2p-1}^{(1)}, b_{2p}^{(1)}, b_{2p+1}^{(1)}, b_{2p+2}^{(1)}, \ldots, b_{2p-1}^{(3)}, b_{2p}^{(3)}, b_{2p+1}^{(3)}, b_{2p+2}^{(3)}),$$

$$\sum_{j=1}^{3} \sum_{m=-1}^{2} [b_{2p+m}^{(j)} \Delta_{ij}(B_{2p+m}(y_{2p+1}))] = F_i(y_{2p+1}, b_{2p}^{(1)}, b_{2p+1}^{(1)}, b_{2p+2}^{(1)}, \ldots, b_{2p-1}^{(3)}, b_{2p}^{(3)}, b_{2p+1}^{(3)}, b_{2p+2}^{(3)}) \quad (p = \overline{0, N};\ i = 1, 2, 3) \tag{10}$$

and from (8) we similarly obtain at the edges:

$$\sum_{j=1}^{3} \sum_{i=-1}^{1} b_i^{(j)} Q_{mj} = L_m(x_0, b_{-1}^{(1)}, b_0^{(1)}, b_1^{(1)}, \ldots, b_{-1}^{(3)}, b_0^{(3)}, b_1^{(3)}),$$

$$\sum_{j=1}^{3} \sum_{i=2N}^{2N+2} b_i^{(j)} P_{mj} = K_m(x_{2N+1}, b_{2N}^{(1)}, b_{2N+1}^{(1)}, b_{2N+2}^{(1)}, \ldots, b_{2N}^{(3)}, b_{2N+1}^{(3)}, b_{2N+2}^{(3)}) \quad (m = 1, 2, 3), \tag{11}$$

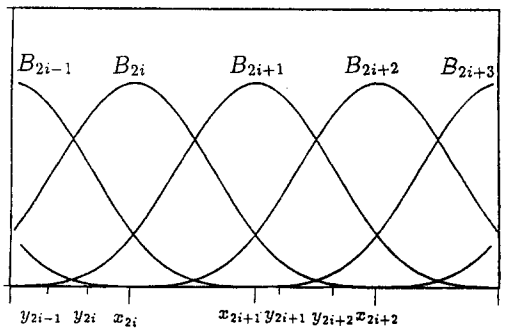

Fig. 2. Choice of nodes of B-splines x_i and collocation points y_i.

where Q_{mj}, L_m, P_{mj}, K_m are determined by the type of boundary conditions under consideration. It should be noted that approximation of the boundary conditions by B-splines does not encounter any special problems, since cubic splines ensure a high degree of accuracy for presenting the first derivative. Relations (10) and (11) yield a system of nonlinear algebraic equations of the order $3(2N+4)$

$$A \cdot \zeta = H(\zeta), \tag{12}$$

where $\zeta^{\mathrm{T}} = (b_{-1}^{(1)}, b_{-1}^{(2)}, b_{-1}^{(3)}, \ldots, b_{2N+2}^{(1)}, b_{2N+2}^{(3)})$, A is a sparse band matrix, with a width equal to 17 and the H-vector represents coordinates, which are nonlinear functions of the ζ components. Furthermore, the system (12) is solved by a method based on a combination of the continuation parameter and Newton methods, which converts the algebraic set into a linear sequence. In accordance with Ortega and Poole (1981) this is solved by iterations for which the kth iteration is obtained as follows:

(1) Solve the system

$$[A - H'(\zeta^{(k)})]\eta^{(k)} = H(\zeta^{(k)}) - A \cdot \xi^{(k)}. \tag{13}$$

(2) Set

$$\zeta^{(k+1)} = \xi^{(k)} + \eta^{(k)}. \tag{14}$$

This process is continued until the condition

$$\left\| \frac{(\zeta^{(k+1)} - \zeta^{(k)})}{\zeta^{(k)}} \right\| < \varepsilon \tag{15}$$

is reached, where ε is of a small prescribed magnitude: $\|\cdot\|$ is one of the norms in the space $\mathscr{R}^{3(2N+4)}$ of $3(2N+4)$-dimensional vectors. In the present calculations ε was set equal to $\varepsilon = 10^{-5}$, and (12) is solved by the Gauss method, utilizing compact band matrix stacking schemes.

In the computer program the forming of an initial estimation $\zeta^{(0)}$, which is "close" to the real solution, is ensured by application of the continuation parameter method. The process begins with small magnitudes of the loading parameter, λ, where the nonlinear solution is close to the linear one. Repeating the calculations for increasing magnitudes of the loading parameter $\lambda_1 + \Delta\lambda_1$, $\lambda_1 + 2\Delta\lambda_1, \ldots$ an initial vector $\zeta^{(0)}$, for each following step, is built by extrapolation of previous solutions. Twice continuously differential cubic splines were used for this purpose.

Within the framework of the present algorithm, determination of singular point positions requires that $\det|A - H'| = 0$ (Andrew *et al.*, 1988). Investigation of the matrix $J_\lambda = |(A - H')(\partial(A - H)/\partial\lambda)|$ is necessary to determine the character of a singular point. If $\det|A - H'| = 0$ and $\det J_k = 0$, a bifurcation point is obtained. On the other hand, if $\det|A - H'| = 0$ and $\det J_k \neq 0$, a limit point is yielded. Here J_k is the matrix obtained from J_λ, after elimination of the kth column. Once the singular points are allocated, further analysis of the postcritical behavior of the deformed state requires the solution of the branching equations (Andreev *et al.*, 1988). Herein, postcritical behavior is investigated only for cases associated with a limit point. The initial segment of the postcritical branch is constructed as follows. An initial estimation of the postlimit solution, $\Delta\lambda < 0$, is obtained by extrapolation of the segment terminated by the last converged prelimit point (the segment size is dictated by extrapolation order). Now, this estimation is employed to find the "exact" solution of (7) by the Newton iteration procedure. Sufficient points of the postlimit branch, which are required to establish the segment size for further extrapolation, are obtained by the same procedure for additional increments $\Delta\lambda$. Then, the successive advance along the branch is realized by application of the extrapolation scheme to the obtained postcritical segment for determining $\xi^{(0)}$, followed by the Newton method for the solution of (12). This

is continued till the lower critical point is achieved. Further, the procedure is repeated for the positive increments of the λ parameter.

The above spline-collocation approach can easily be applied to systems of differential equations with coefficients having first-order finite discontinuities. To ensure fast convergence in such cases it is required to choose the collocation points so that the discontinuities are located between two nodes of the grid δ, which are very close to one another. The scheme used in obtaining the solution in these cases is identical with that used for smooth continuous coefficients. Consequently, the spline-collocation method can also be used to solve problems dealing with stiffened constructions, as well as structures having nonsmooth mechanical parameters.

The above proposed solution technique yields a second order accuracy for any δ. However, theoretical estimation of the accuracy is rather complicated and can be more easily found on the basis of applying the method to a concrete problem and testing the convergence for that particular case.

It is worthwhile noting that in contrast to the finite-difference methods, where the solution is determined only at the nodes of the grid, the spline-collocation method, like finite-elements, provides an approximate solution over the entire interval $[-\alpha_0, \alpha_0]$.

4. RESULTS AND DISCUSSION

Using the present analysis and proposed solution technique responses corresponding to the following cases: stiffened and unstiffened panels subjected to pressure only; unstiffened panels exposed to heating alone and to combined heating and pressure, were investigated.

4.1. *Verification test calculations*

In order to assess the capability of the proposed approach to predict adequately the panel response, verification calculations were performed prior to its application for the solution of the above loading cases.

4.1.1. *Simply-supported isotropic panel under pressure* (h/R = 1/10; 1/100; 1/1000; $\alpha_0 = 1/2\sqrt{6(h/R)}$) *—comparison with Grigorenko* (1977). A rigorous exact solution (Grigorenko, 1977) yields a nondimensional "critical" deflection:

$$w^* = -2/3h \cdot w(0)$$

and "critical" pressure

$$q^* = -18(R/h)^2[(1-\nu^2)/E]q.$$

Results obtained by the present analysis for upper and lower critical loads, together with the corresponding deflections at panel midpoint, are given in Table 1. It is apparent from Table 1 that "classical" theory yields results which are h/R independent, whereas taking into account transverse shear significantly affects the results. This is particularly emphasized when comparing the values w_L^* and q_L^* yielded by the "classical" model with those obtained by the present analysis for the relatively thick panel, $h/R = 1/10$.

Table 1. Critical loads and deflections—verification tests

	Proposed approach				Grigorenko (1977) ("classical" model)			
h/R	q_u^*	w_u^*	q_L^*	w_L^*	q_u^*	w_u^*	q_L^*	w_L^*
1/10	2.86523	0.31334	1.49984	0.77960				
1/100	2.95803	0.31765	1.91898	0.72238	2.96984	0.31820	1.96752	0.71680
1/1000	2.96621	0.31783	1.95721	0.71688				

u—upper; L—lower.

Table 2. Effect of type of discretization on convergence of $q_u \cdot 10^{-7}$ (Pa)

N	10	25	50	100	150	200	300	600
$x_i = y_i$	6.46922	6.38949	6.37754	6.37449	6.37392	6.37372	6.37357	6.37349
$x_i \neq y_i$	6.34533	6.36824	6.37211	6.37312	6.37331	6.37337	6.37342	6.37345

4.1.2. *Convergence—clamped orthotropic panel under pressure* ($R = 1$ m; $h = R/10$; $\alpha_0 = \pi/6$; $\nu_{12} = 0.1742$; $\nu_{21} = 0.1057$; $E_2 = 2.808 \cdot 10^{10}$ Pa; $G_{23} = E_2/10$). Convergence of the proposed method, Section 3, is tested for two different cases of the domain discretization: (a) the collocation points, y_i, coincide with nodes of B-splines, x_i, and (b) $x_i \neq y_i$. The results of calculations of the upper critical load $q_u \cdot 10^7$ and of er (w), the relative deviation from the exact solution (w calculated at the midpoint), obtained for various discretizations N, are presented in Table 2 and Fig. 3. It is apparent both from Table 2 and Fig. 3, that the choice $x_i \neq y_i$ yields faster convergence and that the critical load converges faster than the deflection, w. Furthermore, it is seen that for the case $x_i = y_i$ the convergence is approached from above, whereas for $x_i \neq y_i$ it is approached from below.

The results of Fig. 3 are corroborated by those obtained in Sheinman and Adan (1987), where a finite difference scheme is applied, and it is demonstrated that convergence depends upon the load level, i.e. convergence in the linear region of the load-deflection diagram is achieved with considerably fewer discrete points than in the highly nonlinear region.

4.1.3. *Convergence—clamped stiffened panel under uniform normal pressure* ($R = 30 \cdot h$; $h = 1$ mm; $\alpha_0 = \pi/8$; *four equidistant stiffeners*: *stiffener height*, $h_s = 0.3 \cdot h$; *stiffener width*, $t_s = 1.2 \cdot h$ *and mechanical properties of example* 4.1.2). Due to the presence of stiffeners the panel thickness is piecewise continuous and the values of C_{ij}, K_{ij}, D_{ij}, N_{iT} and M_{iT} undergo abrupt changes in stations, where a stiffener starts and terminates. To account for these abrupt changes and to overcome anticipated convergence problems a considerably refined discretization scheme was used in the vicinity of a skin-stiffener transition. It should be noted that the present analysis treats the stiffeners, as well as the geometry and properties of the skin-stiffener combination as being "smeared" [see Baruch and Singer (1963)]. Therefore, to avoid discrete effects and to provide adequate and satisfactory results, the stiffeners in the present verification study are light to moderate and closely spaced.

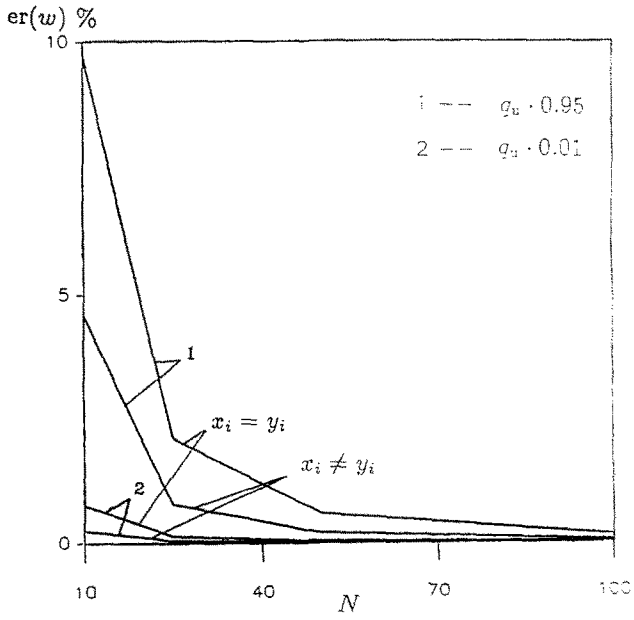

Fig. 3. Convergence of w at midpoint.

Table 3. Effect of stiffening on convergence

	Internal stringers			External stringers			Unstiffened panel
	$-w/h \cdot 10^3$			$-w/h \cdot 10^3$			
N	$q = -10^4$ (Pa)	$q = -7.71 \cdot 10^6$ (Pa)	$-q_u \cdot 10^{-6}$ (Pa)	$q = -10^4$ (Pa)	$q = -7.71 \cdot 10^6$ (Pa)	$-q_u \cdot 10^{-6}$ (Pa)	$-q_u \cdot 10^{-6}$ (Pa)
41	0.4800	693.37	7.989	0.4732	690.23	8.342	7.0896
82	0.4825	748.35	7.825	0.4755	714.40	8.233	7.0974
164	0.4836	788.75	7.758	0.4766	725.28	8.146	7.0994
328	0.4836	795.76	7.751	0.4769	726.75	8.145	7.0998

Internal and external stiffening were examined in the present test and convergence of the critical loads and associated midpoint deflections are presented in Table 3. It appears that the presence of stiffeners affects the solution and a relatively large number of collocation points (fine mesh) is required to minimize the relative convergence error. Also, as expected, externally stiffened panels are more efficient, i.e. they yield higher upper critical loads and lower critical deflections than internally stiffened panels do. There is also a significant difference between the postbuckling behavior of externally and internally stiffened panels. This will be discussed in the next section.

It is worthwhile noting that in all of the above test cases the maximum number of iterations, that were required for each increment of load $\Delta\lambda$, were mesh size independent. They did not exceed 5 for achieving a convergence of $\varepsilon = 10^{-6}$, per step, even in the most nonlinear intervals of behavior. This is also true for the results presented and discussed in the next section.

4.2. *Normal uniform pressure—unstiffened and stiffened panels*

Numerous studies dealt with these problems [e.g. see Yamaki (1984), Shreyer and Masur (1966) and Sheinman and Frostig (1988)], however most of them neglect transverse shear effects. As shown in Sheinman and Adan (1987) this may lead to erroneous results and conclusions.

4.2.1. *Unstiffened panels.* Shear effects measured by the moduli ratio, G_{230}/E_{20}, were studied on the response of the panel in 4.1.2, with clamped boundary conditions, for the following moduli ratios $G_{230}/E_{20} = 1/(2(1+\nu_{12}))$, 0.1 and 0.01. The results are demonstrated in Fig. 4. The upper and lower critical loads are reduced considerably and the

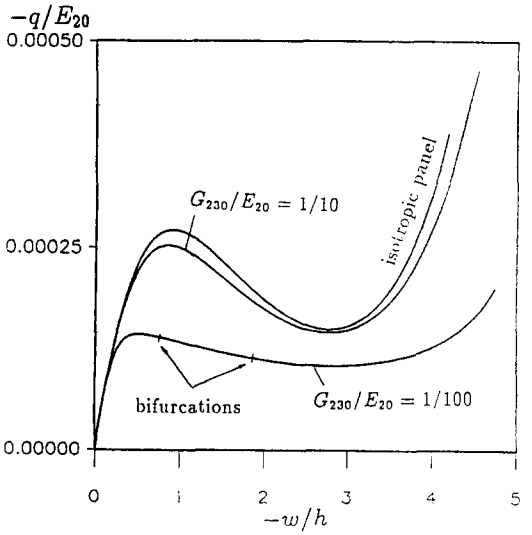

Fig. 4. Effect of transverse shear, G_{230}/E_{20}—clamped panel.

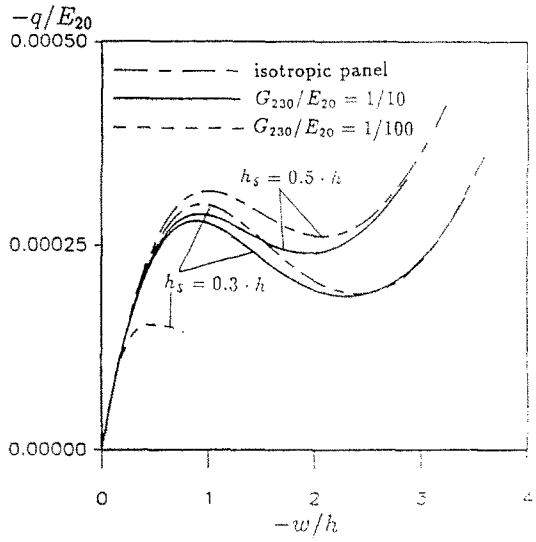

Fig. 5. Load-deflection curves—internally stringer-stiffened clamped panel.

postbuckling behavior, associated with a large transverse shear effect, differs significantly from that experienced with a small shear effect. This is reflected by the significant reduction in the difference between the upper and lower critical loads with increase in the G_{230}/E_{20} ratio. Also, it was found as well as observed in Fig. 4 that two bifurcation points exist in the postbuckling zone only for small values of G_{230}/E_{20}. However, they do not influence the symmetric mode of buckling. Contrary to this behavior, additional calculations showed that an identical simply-supported panel experiences two bifurcation points for all tested values of G_{230}/E_{20}, but the first one is achieved prior to the upper critical load and is associated with an asymmetric buckling mode.

4.2.2. *Stiffened panels.* The results obtained for the internally stiffened panels of 4.1.3 are depicted in Fig. 5 and those yielded for externally stiffened ones in Fig. 6. The combined effects of stringer height and transvere shear are also studied in these figures. It is observed in these figures that the postbuckling behavior of stringer-stiffened panels depends upon location of stiffeners. Furthermore, Fig. 6 suggests that since either the difference between

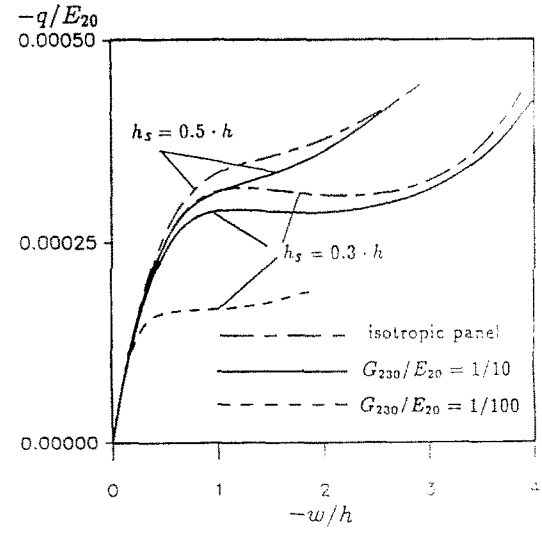

Fig. 6. Load-deflection curves—externally stringer-stiffened clamped panel.

the upper critical load, q_u, and lower critical load, q_L, is very small, or snap-through does not exist, externally stiffened panels are less sensitive to the presence of initial geometric imperfections than internally stiffened panels, which experience snap-through (Fig. 5). Hence, due to their reduced "sensitivity", externally stiffened panels are considerably more structurally efficient than internally stiffened ones.

Examining the transverse shear effect it appears from both Fig. 5 and Fig. 6 that isotropic panels sustain the highest critical loads. These figures demonstrate and emphasize, therefore, that neglect of transverse shear may result in significant overestimation of the load carrying capacity. It is seen from Figs 5 and 6 that q_u of a panel with $G_{230}/E_{20} = 0.01$ is only about 50% of that corresponding to an isotropic panel.

4.3. *Thermal postbuckling behavior*

In this section the temperature dependence of material properties, E_i, G_{23} and α_i^*, in addition to transverse shear, is accounted for in the analysis of the panels. It should be noted that whereas among the many studies on thermal buckling temperature dependent material properties are included only in a few of them [e.g. Krysko and Fedorov (1984)], there are no practically, postbuckling studies which include this temperature dependency.

4.3.1. *Simply-supported shallow panel nonuniformly heated through the thickness* ($h = 1$ mm; $R = 700 \cdot h$; $\alpha_0 = \pi/72$). The temperature-dependent properties and coefficients (Section 2) for this example are as follows: $E_{20} = 2.808 \cdot 10^{10}$ Pa; $G_{230} = E_{20}/3$; $\nu_{12} = 0.1742$; $\nu_{21} = 0.1057$; $\alpha_{10} = 0.1134 \cdot 10^{-4}$ °C^{-1}; $\alpha_{20} = 0.1418 \cdot 10^{-4}$ °C^{-1}; $b_{12} = 0.25 \cdot 10^{-2}$ °C^{-1}; $g_{12} = b_{12}$; $l_{11} = 0.2413 \cdot 10^{-7}$ °C^{-1}; $l_{12} = 0.2445 \cdot 10^{-7}$ °C^{-1}; $b_{21} = g_{2i} = l_{2i} = 0$ $(i = 1, 2)$.

Under the present nonuniform heating, a bending moment M_{2T}, leading to buckling, is induced. The response of a panel, fabricated from a temperature-independent material, is compared with that of a temperature-dependent material in Fig. 7. It is observed in this figure that accounting for $E_i(T)$, $G_{i3}(T)$ and $\alpha_i^*(T)$ in the analysis leads to significant reduction in the load carrying capacity of the panel. It can sustain only about half the bifurcation load carried by a panel for which temperature dependence of material properties is discarded. On the other hand, it is apparent from Fig. 7 that the second bifurcation point is almost identical in both cases of calculations. Also, it is found within the framework of the present model that for the type of heating considered herein buckling occurs only for shallow panels and provided that a considerable change in temperature exists between the upper and lower surface of the panel.

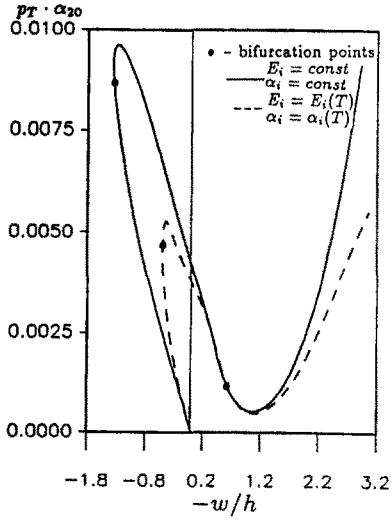

Fig. 7. Load-deflection curves—simply-supported shallow panel subjected to nonuniform through the thickness heating $T = (-1.3 \cdot z/h + 0.35) \cdot p_T$.

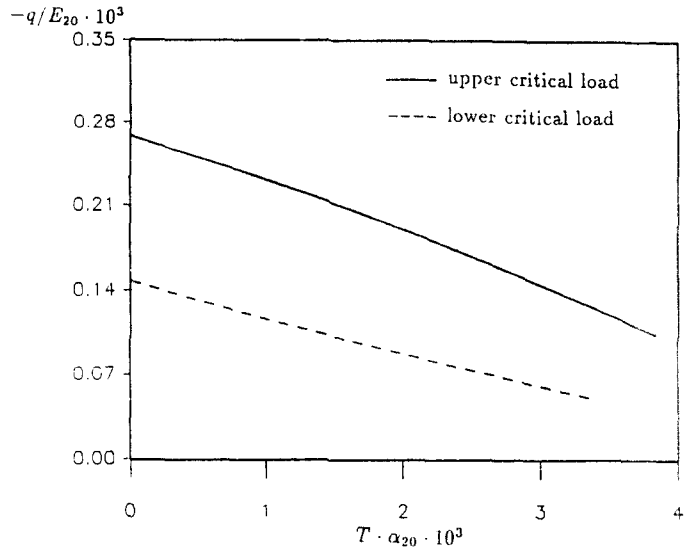

Fig. 8. Buckling interaction curves—clamped panel under combined pressure and uniform heating (including temperature dependence of material properties).

4.3.2. *Clamped panel subjected to combined uniform pressure and heating* ($h = 1$ mm; $R = 30 \cdot h$; $\alpha_0 = \pi/8$). The interaction curves corresponding to the nondimensional upper and lower critical loads versus nondimensionalized temperature $T \cdot \alpha_{20} \cdot 10^3$, are shown in Fig. 8. The temperature dependent properties are identical with those of example 4.3.1. The depicted graphs are almost linear and it appears that elevation in temperature drastically affects the load sustained by the panel. It should be emphasized that neglect of the temperature dependence of material properties in the analysis yields results which are practically temperature independent, i.e. the interaction curve will remain almost horizontal. Hence, failure to account for $E_i(T)$, $G_{i3}(T)$ and $\alpha_i^*(T)$ may lead to considerable overestimation of the loads withstood by the panel and consequently to erroneous decisions in the design of structures exposed to aerothermal loading.

5. CONCLUSIONS

(1) An analysis, for studying the pre- and postbuckling response of stiffened and unstiffened infinite length cylindrical panels with various boundary conditions and subjected to thermal and mechanical loads, was developed.
(2) Transverse shear effects and temperature dependence of elastic moduli and of thermal expansion coefficients were included in the analysis.
(3) A spline-collocation method was applied for solving the system of highly nonlinear differential equations pertinent to the present boundary problem.
(4) Verification test calculations were performed to assess the accuracy and adequacy of the proposed analysis. Good correlation with rigorous exact solutions is demonstrated.
(5) Convergence studies indicated that the fastest convergence is achieved when collocation points do not coincide with the nodes of B-splines.
(6) Isotropic panels sustain the highest critical pressures. Therefore, neglect of transverse shear effects may result in overestimation of the load carrying capacity of the panel.
(7) Accounting for transverse shear effects and temperature-dependent properties may lead to a significant reduction in the loads sustained by a panel in comparison with "classical" results.
(8) Analysis of postbuckling behavior of stiffened panels subjected to pressure loading

indicated that externally stiffened panels are less "sensitive" to initial imperfections and are more structurally efficient.

(9) Failure to account for $E_i(T)$, $G_{i3}(T)$, $\alpha_i^*(T)$ may lead to considerable overestimation of the loads withstood by the panel.

Acknowledgements—The authors would like to express their thanks to Professor J. Singer for his helpful discussions and suggestions. Igor Patlashenko was sponsored by the Center of Absorption in Science, Ministry of Immigrant Absorption, Israel.

REFERENCES

Andreev, L. V., Obodan, N. I. and Lebedev, A. G. (1988). *Stability of Nonsymmetric Shell Deformation.* Nauka, Moscow.

Baruch, B. and Singer, J. (1963). Effect of eccentricity of stiffeners on the general instability of stiffened cylindrical shells under hydrostatic pressure. *J. Mech. Engng Sci.* **5**(1), 23–27.

Grigorenko, Ya. M. (1977). About the solution of deformation problem of flexible long cylindrical shell with variable parameters. *Dokl. Akad. Nauk. Ukr. SSR* **Ser. A,** No. 5, 418–422 (in Ukrainian).

Grigorenko, Ya. M. and Timonin, A. M. (1982). Numerical solution of nonaxisymmetrical problems in the nonlinear theory of laminated shells of revolution. *Prikl. Mekh.* **18**(5), 43–48.

Jackson, L. R., Dixon, S. C., Tenney, D. R., Carter, A. L. and Stephens, J. R. (1987). Hypersonic structures and materials: A progress report. *Aero. Am.* Oct. 1987, 24–30.

Keene, F. W. and Hetnarsky, R. B. (1990). Bibliography on thermal stresses. *J. Therm. Stress.* **13**(4), 343–542.

Khoroshun, L. P., Kozlov, S. V. and Patlashenko, I. Yu. (1988a). Determination of the axisymmetric stress–strain state of heat-sensitive shells of revolution by the spline-collocation method. *Prikl. Mekh.* **24**(6), 56–63.

Khoroshun, L. P., Kozlov, S. V. and Patlashenko, I. Yu. (1988b). Stress–strain state of thermosensitive variable thickness shells of revolution. *Prikl. Mekh.* **24**(9), 38–44.

Krysko, V. A. and Fedorov, P. B. (1984). Study of the dynamic stability of a shallow shell in relation to mechanical and thermal characteristics. *Prikl. Mekh.* **20**(3), 44–48.

Ortega, J. M. and Poole, W. G. (1981). *An Introduction to Numerical Methods for Differential Equations.* Pitman Publishing Inc., Marshfield.

Sheinman, I. and Adan, M. (1987). The effect of shear deformation on post-buckling behavior of laminated beams. *ASME J. Appl. Mech.* **54,** 558–562.

Sheinman, I. and Frostig, J. (1988). Post-buckling analysis of stiffened laminated panel. *ASME J. Appl. Mech.* **55,** 635–640.

Shih, P. K., Pruntyu, J. and Mjueller, R. N. (1988). Thermostructure concepts for hypervelocity vehicles. Proc. AIAA/ASME/ASCE/AHS/ASC 29th Structures, Structural Dynamics and Material Conference, paper No. 88-2295.

Shreyer, H. L. and Masur, E. F. (1966). Buckling of shallow arches. *J. Engng Mech. Div., ASCE,* No. EM4, Proc. paper 4875, pp. 1–19.

Tenney, D. R., Lisagor, W. B. and Dixon, S. C. (1988). Materials and structures for hypersonic vehicles. ICADS Paper 88-2.3.1, Jerusalem, Israel, pp. 398–415.

Thornton, E. A. (1990). Thermal structures: Four decades of progress. Proc. AIAA/ASME/ASCE/AHS/ASC 31st Structures, Structural Dynamics and Material Conference, paper No. 90-0971.

Thornton, E. A. and Dechaumphai, P. (1987). Coupled flow, thermal and structural analysis of aerodynamically heated panels. Proc. AIAA/ASME/ASCE/AHS/ASC 28th Structures, Structural Dynamics and Material Conference, paper No. 87-0700.

Thornton, E. A., Oden, J. T., Tworzydslo, W. W. and Youn, S. K. (1989). Thermoviscoplastic analysis of hypersonic structures subjected to severe aerodynamic heating. Proc. AIAA/ASME/ASCE/AHS/ASC 30th Structures, Structural Dynamics and Material Conference, paper No. 89-1226.

Wieting, SA. R., Dechaumphai, P. and Bey, K. S. (1988). Application of integrated fluid-thermal-structural analysis methods. ICAS Paper 88-2.3.3, Jerusalem, Israel, pp. 424–434.

Yamaki, N. (1984). *Elastic Stability of Circular Cylindrical Shells.* North-Holland, Amsterdam.

Zav'yalov, Yu. S., Kvasov, B. I. and Miroshnichenko, V. L. (1980). *Methods of Spline-Functions.* Nauka, Moscow.

Ziegler, F. and Rammerstorfer, F. G. (1989). Thermoelastic stability. In *Thermal Stresses III* (Edited by R. B. Hetnarsky), pp. 107–191. North-Holland, Amsterdam.

APPENDIX

The differential operators Δ_{ij} and the nonlinear functions F_i in (7) are determined by the following expressions:

$$\Delta_{11} = \frac{1}{R^2}\left[\left(C_{22} - \frac{1}{R}K_{22}\right)\frac{d^2}{d\alpha_2^2} + \left(C_{22,2} - \frac{1}{R}K_{22,2}\right)\frac{d}{d\alpha_2} + \left(C_{22,2} - \frac{1}{R}K_{22,2}\right)\right],$$

$$\Delta_{12} = \frac{1}{R^2}\left[\left(C_{22} + C_{23} - \frac{1}{R}K_{22} - N_{2T} - \frac{1}{R}M_{2T}\right)\frac{d}{d\alpha_2} + \left(C_{22,2} - \frac{1}{R}K_{22,2}\right)\right],$$

$$\Delta_{13} = \frac{1}{R^2}\left[K_{22}\frac{d^2}{d\alpha_2^2} + K_{22,2}\frac{d}{d\alpha_2} + R\cdot C_{23}\right],$$

$$\Delta_{21} = \frac{1}{R^2}\left[\left(\frac{1}{R}K_{22} - C_{23} - C_{22} + N_{2T} + \frac{1}{R}M_{2T}\right)\frac{\mathrm{d}}{\mathrm{d}\alpha_2} + \left(N_{2T,2} + \frac{1}{R}M_{2T,2} - C_{23,3}\right)\right],$$

$$\Delta_{22} = \frac{1}{R^2}\left[\left(C_{23} - N_{2T} - \frac{1}{R}M_{2T}\right)\frac{\mathrm{d}^2}{\mathrm{d}\alpha_2^2} + \left(C_{23,2} - N_{2T,2} - \frac{1}{R}M_{2T,2}\right)\frac{\mathrm{d}}{\mathrm{d}\alpha_2} + \left(\frac{1}{R}K_{22} - C_{22}\right)\right],$$

$$\Delta_{23} = \frac{1}{R^2}\left[(R\cdot C_{23} - K_{23})\frac{\mathrm{d}}{\mathrm{d}\alpha_2} + R\cdot C_{23,2}\right],$$

$$\Delta_{31} = \frac{1}{R^2}\left[\left(K_{22} - \frac{1}{R}D_{22}\right)\frac{\mathrm{d}^2}{\mathrm{d}\alpha_2^2} + \left(K_{22,2} - \frac{1}{R}D_{22,2}\right)\frac{\mathrm{d}}{\mathrm{d}\alpha_2} + R\cdot C_{23}\right],$$

$$\Delta_{32} = \frac{1}{R^2}\left[\left(K_{22} - \frac{1}{R}D_{22} - R\cdot C_{23}\right)\frac{\mathrm{d}}{\mathrm{d}\alpha_2} + \left(K_{22,2} - \frac{1}{R}D_{22,2}\right)\right],$$

$$\Delta_{33} = \frac{1}{R^2}\left[D_{22}\frac{\mathrm{d}^2}{\mathrm{d}\alpha_2^2} + D_{22,2}\frac{\mathrm{d}}{\mathrm{d}\alpha_2} - R^2\cdot C_{23}\right],$$

$$F_1 = \frac{1}{R}N_{2T,2} - q_2^* - \frac{1}{R^3}\left[\frac{\mathrm{d}}{\mathrm{d}\alpha_2}\left(C_{22}\left(\frac{1}{2}v^2 + \frac{1}{2}\left(\frac{\mathrm{d}w}{\mathrm{d}\alpha_2}\right)^2 - v\cdot\frac{\mathrm{d}w}{\mathrm{d}\alpha_2}\right)\right)\right] + \frac{1}{R^3}\left(v - \frac{\mathrm{d}w}{\mathrm{d}\alpha_2}\right)\left[\left(C_{22} - \frac{1}{R^2}D_{22}\right)\left(\frac{\mathrm{d}v}{\mathrm{d}\alpha_2} + w\right)\right.$$
$$\left. + \left(K_{22} + \frac{1}{R}D_{22}\right)\frac{\mathrm{d}\psi_2}{\mathrm{d}\alpha_2} + \left(\frac{1}{R}C_{22} + \frac{1}{R^2}K_{22}\right)\left(\frac{1}{2}v^2 + \frac{1}{2}\left(\frac{\mathrm{d}w}{\mathrm{d}\alpha_2}\right)^2 - v\cdot\frac{\mathrm{d}w}{\mathrm{d}\alpha_2}\right)\right],$$

$$F_2 = -\frac{1}{R}N_{2T} - q_3^* + \frac{1}{R^3}\left[C_{22}\cdot\left(\frac{1}{2}v^2 + \frac{1}{2}\left(\frac{\mathrm{d}w}{\mathrm{d}\alpha_2}\right)^2 - v\cdot\frac{\mathrm{d}w}{\mathrm{d}\alpha_2}\right)\right] + \frac{1}{R^3}\frac{\mathrm{d}}{\mathrm{d}\alpha_2}\left[\left(v - \frac{\mathrm{d}w}{\mathrm{d}\alpha_2}\right)\left(\left(C_{22} - \frac{1}{R^2}D_{22}\right)\left(\frac{\mathrm{d}v}{\mathrm{d}\alpha_2} + w\right)\right.\right.$$
$$\left.\left. + \left(K_{22} + \frac{1}{R}D_{22}\right)\frac{\mathrm{d}\psi_2}{\mathrm{d}\alpha_2} + \left(\frac{1}{R}C_{22} + \frac{1}{R^2}K_{22}\right)\left(\frac{1}{2}v^2 + \frac{1}{2}\left(\frac{\mathrm{d}w}{\mathrm{d}\alpha_2}\right)^2 - v\cdot\frac{\mathrm{d}w}{\mathrm{d}\alpha_2}\right)\right)\right],$$

$$F_3 = \frac{1}{R}M_{2T,2} - \frac{1}{R^3}\frac{\mathrm{d}}{\mathrm{d}\alpha_2}\left[K_{22}\left(\frac{1}{2}v^2 + \frac{1}{2}\left(\frac{\mathrm{d}w}{\mathrm{d}\alpha_2}\right)^2 - v\cdot\frac{\mathrm{d}w}{\mathrm{d}\alpha_2}\right)\right],$$

where $(\,)_{,2} = \mathrm{d}(\,)/\mathrm{d}\alpha_2$.